

Assessment of Multilayered Plates with Hyperelastic Coatings Subjected to Dynamic Loadings by Impact at Low Velocities

FLORINA BUCUR, LIVIU-CRISTIAN MATACHE*

Military Technical Academy „Ferdinand I”, 39-49 G. Coșbuc Av., 040531, Bucharest, Romania

Abstract: *This paper describes the use of video and digital image processing in investigation of the impact between a rigid hemispherical shape impactor and Hybrid Polyurea-Polyurethane-MWCNTs Nanocomposite Coatings. An experimental study was performed for six sample configurations: single aluminum plates (reference test), multilayer plates with 4 types of coatings and double aluminum plates. The impact phenomenon was recorded with a high-speed video camera and the variation of the projectile's velocity during the impact was obtained through digital analysis. Additionally, the test was instrumented using a force sensor specially designed and mounted on the impactor. The video processing was used to draw the velocity curves and to estimate the evolution of the contact forces between the impactor and the multilayer structures, the results obtained being compared with the force sensor data. Some differences between these two types of measurements are observed, so in order to analyze the configurations behavior, a numerical study of the phenomena was performed in LS-DYNA software using a 2D axial symmetric model. The simulations showed that the profile of the force evolution measured with the sensor is affected by the chosen constructive solution and the data obtained based on the video images are more accurate. The deformations were analyzed, the maximum deformation based on image processing and the residual deformation based on 3D Scan post-test. The video technique combined with 3D Scan are precise enough to study the impact at low velocities and the numerical simulations provide results according to reality. The hyperelastic coatings contribute to a better resistance of the aluminum plates.*

Keywords: *polyurea-polyurethane, multiwall carbon nanotubes, coatings, 3D Scan, video image processing, impact, numerical simulation*

1. Introduction

Lately, the development of lightweight configurations based on metal – hyperelastic material combinations used in ballistic protection applications has been intensively studied.

The scientific literature presents many studies where is highlighted the potential of polyurea, as the most common hyperplastic material, to enhance the mitigation of dynamic and impulsive loads by different materials and structures when is used in various combinations [1-5].

A large number of papers refers to the polyurea coatings on structures used to mitigate blast and impact effects, especially for decreasing the damaging effect on structures used for individual or collective ballistic protection [6-13].

Moreover, the research also extended towards the study of different polyurea synthesis with improved physical and mechanical properties and, also, location combinations (in the front, in the middle or on the back of tested configurations) [5, 11-12].

Besides the study of coated steel plates, the potential of polyurea to be used as protection layer for aluminum plates and its behavior when is subjected to low velocities and high velocities impact loadings was approached [13-17].

At the same time, the polyurea properties improvement was investigated and, namely, polyurea-polyurethane-nanocomposite coatings for ballistic protection have been the subject of several papers [4, 18-20].

*email: liviu.matache@mta.ro

Another exploited direction refers to the testing methods and also test instrumentation procedures for specific parameters measurement and the results processing.

In this regard, for a better understanding of materials behavior, during the experimental tests (mechanical testing, ultrasonic testing), different types and configurations of samples and measurement tools have been tested (simple/bilayer/multilayer configurations, force or pressure transducers, video-speed cameras, scanning electron microscopy, computed tomography etc.), in static, dynamic or impulsive regime, corroborated with numerical simulation, in order to obtain valid outcomes and results that can be extrapolated to large-scale experiments and applications [13, 20-29].

Regarding the laboratory testing of aluminum-polyurea composite plates, punch indentation [29], impact of low velocity blunt-nosed projectiles [16] or impact of a blunt-nosed hammer [28] were investigated by experiments and numerical simulations.

Also, in terms of test instrumentation, besides classical sensors (transducers), the potential of high-speed photography, digital image correlation methods and X-ray computed tomography (CT), the comparison between experimental data and numerical simulations [13, 19, 21, 26-27], has been investigated.

The possibility to evaluate the behavior of polyurea in different configurations and for different loadings was investigated through numerical simulations with materials models available in computational codes, being obtained results similar to the real ones [11, 13, 25, 30-32].

The present study refers to an experimental and numerical evaluation of a hyperelastic material, namely polyurea-polyurethane-MWCNTs nanocomposite. Aluminum specimens (0.5 mm thickness plates) were coated with an additional layer with 1 mm thickness of simple polyurea-polyurethane and reinforced with multiwall carbon nanotubes in different concentrations (back-side – opposite to impact).

The method for obtaining the polyurea-polyurethane-multiwall carbon nanotubes (MWCNTs) nanocomposites evaluated in this paper is presented in [5, 20]. Also, their potential to be used in impact application due to their improved mechanical properties is demonstrated (the integrity of the aluminum plate coated with nanocomposite layers is maintained at a force value almost 200% higher than for the uncoated standard plates).

The possibility of using 3D scans and video images processing, corroborated with classical force transducer to estimate parameters of interest that characterize the behavior of the multilayer plates, is investigated. The use of experimental video images processing in order to understand how phenomena unfold in laboratory conditions at low velocity, for foam type materials, was already explored [23].

The numerical approach is used to clarify the differences between each type of measurement tools that is used. Using the LS-DYNA software, a 2D axis-symmetric model was created and numerical simulations were performed for each configuration experimentally tested.

The results obtained through numerical simulation validated the experimental ones, the results being consistent.

2. Materials and methods

2.1. Experimental testing

The experimental study is performed at a standard temperature of 25°C, in dynamic regime, in order to analyze the behavior of multilayer configurations at loadings produced at low velocities.

The laboratory testing follows a simple methodology that implies using a pneumatic propulsion system for determining the resistance force resulting from the loading of specimen on impact with a hemispherical shape impactor. Specimens with the same lateral dimension but different structures, single-layer and multilayer, were tested.

The 3D experimental set-up is presented in Figure 1.

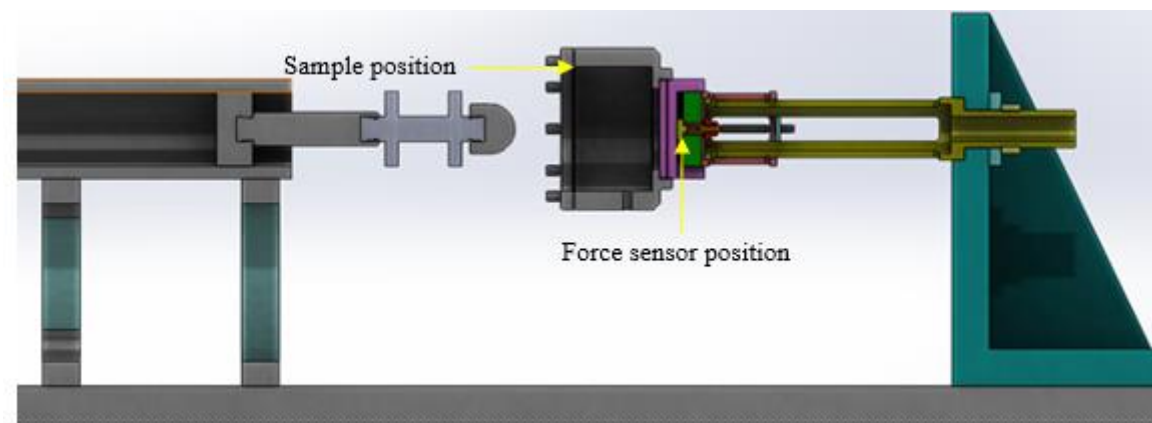


Figure 1. Experimental set-up

The rigid hemispherical impactor (non-deformable) has the head diameter of 40 mm and a mass of 800 g (Figure 2a).

The reference sample used for these tests is represented by an aluminum plate with 2.78 g/cm^3 density, having a thickness of 0.5 mm and a free diameter of 100 mm (Figure 2b).

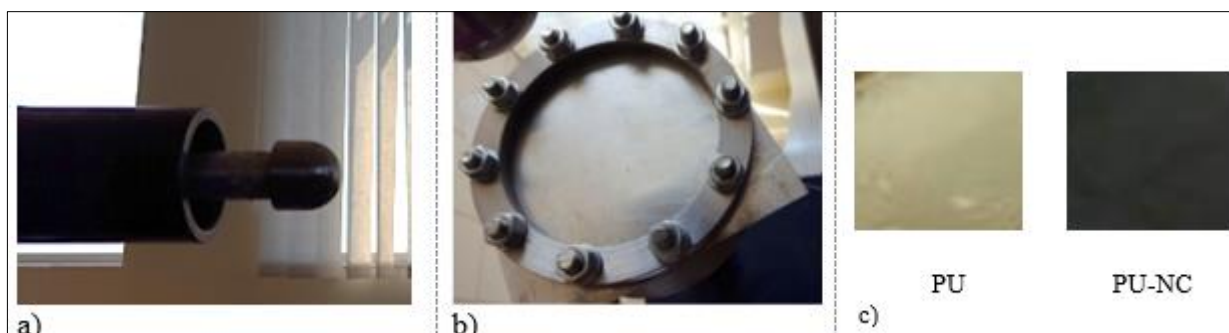


Figure 2. a) hemispherical shape impactor, b) sample prepared for testing, c) polymeric films: PU-simple polyurea-polyurethane, PU-NC-polyurea-polyurethane with nanocomposites

The experimental tests included six series of tests executed at different low velocities impact:

- simple aluminum plate of 0.5 mm thickness –S.A. – 4 tests;
- multilayer plate: aluminum plate (0.5 mm) + simple polyurea-polyurethane with 1 mm thickness – SA+PU – 5 tests;
 - multilayer plate: aluminum plate (0.5 mm) + polyurea-polyurethane-MWCNTs nanocomposite (1 mm black polyurea + carbon nanotubes in a percentage of 0.1%) –SA+ PU-NC2 – 6 tests;
 - multilayer plate: aluminum plate (0.5 mm) + polyurea-polyurethane-MWCNTs nanocomposite (1 mm black polyurea + carbon nanotubes in a percentage of 0.2%) – SA+PU-NC3 – 6 tests;
 - multilayer plate: aluminum plate (0.5 mm) + polyurea-polyurethane-MWCNTs nanocomposite (1 mm black polyurea + carbon nanotubes in a percentage of 0.3%) – SA+PU-NC4 – 6 tests;
 - multilayer plate: double aluminum plates (2 x 0.5 mm) – DA – 6 tests.

The four types of polyurea-polyurethane nanocomposites tested were obtained through a facile synthesis route: multiwall carbon nanotubes (prior pre-dispersed in a polyester polyol matrix) were mixed with two component of amino functional groups and a component of isocyanate functional groups. To ensure the homogenous and uniform dispersion of the nanofiller inside the polymeric matrix the solution was subjected to ultrasound [20].

The synthesized polyurea-polyurethane nanocomposite films (polymeric films, Figure 2c) were subjected to uniaxial tensile tests. The mechanical properties and the description of each type of hyperelastic coating layers used on the aluminum plates are presented in detail in [20].

According to those information and the true-stress curves evolution drawn from it, is point out that the polyurea-polyurethane nanocomposites with 0,2 % MWCNTs has the best properties (Figure 3).

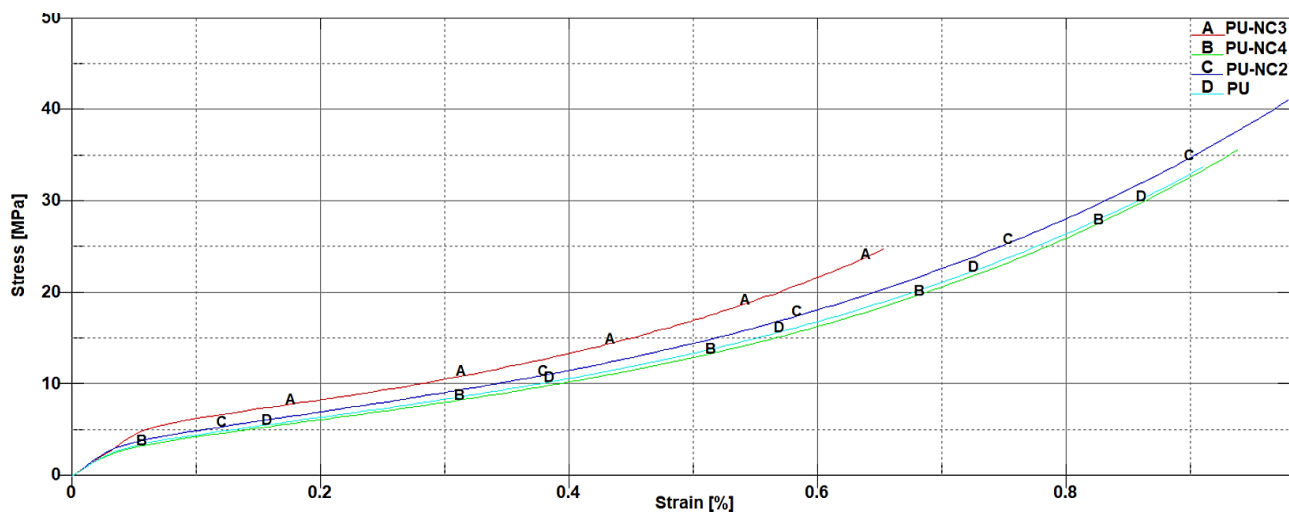


Figure 3. True stress-true strain curves for the polyurea-polyurethane nanocomposite films

To launch the impactor in the direction of the sample center a pneumatic gun was used. Due to the rapid impact and resulting stress, the sample plates suffer permanent deformations, cracks and even fracture (Figure 4).



Figure 4. Aspects from testing a simple aluminum plate [5]

A PCB Piezotronics 200B05 force transducer, attached to a rigid steel support, along with a PCB signal conditioner and a PicoScope®6 series were used. This location was chosen in order to emphasize the resistance of the sample to dynamic loads in the case of using multilayer structures (Figure 5a).

In the same testing configuration, a high-speed camera PHOTRON FASTCAM SA-Z (30,000 fps setting) was used to record experimental tests (Figure 5b).

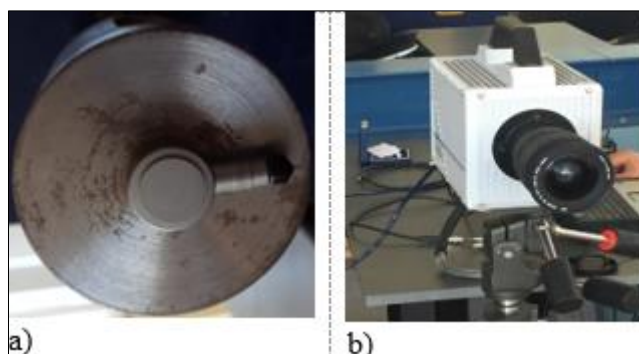


Figure 5. Measuring tools: a) piezoelectric force sensor, b) high-speed video camera

In order to analyze the performed tests, the sensor recorded force, the videos from high-speed camera and 3D scans of tested plates are used.

After laboratory testing, each plate deformation pattern is investigated with a professional-grade 3D scanner, Portable 3D ScannerGo! (a Creaform ACADEMIA™ solution) [33]. This device and its technology allow the capture of high-quality geometries and accurate measurements. Some sequences from the 3D scanning operation are presented in Figure 6.

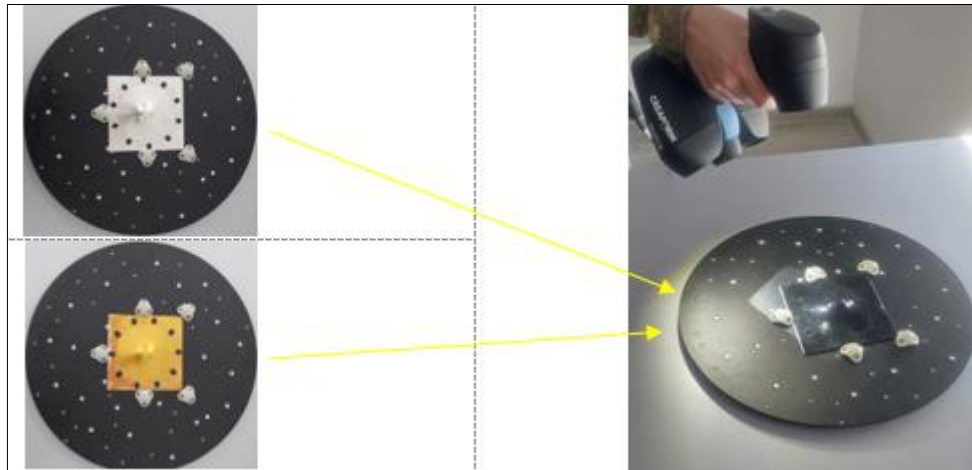


Figure 6. Sequences from 3D scanning operation

The 3D scans are evaluated by VXmodel, a post-processing software that integrates VXelements, a 3D scanning platform that allows the captured 3D scan data to be investigated for further measurements [34].

In Figure 7, the program interface and a model of deformation measurement are illustrated.

All tested plates, had been evaluated to determine the residual deformation after impact, and the data obtained are presented in Section 3.

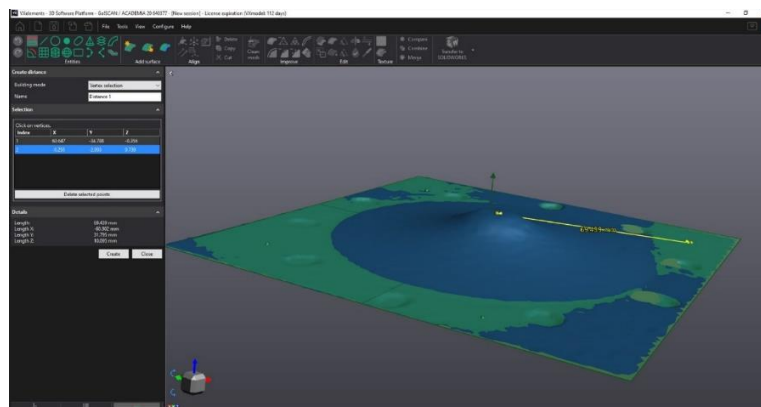


Figure 7. 3D scan processing

The videos recorded are investigated with Tracker software (Figure 8). The displacement for three distinct points is recorded and the data are exported and processed through Mathcad software, using an algorithm to determine the velocity, the acceleration and the maximum force.

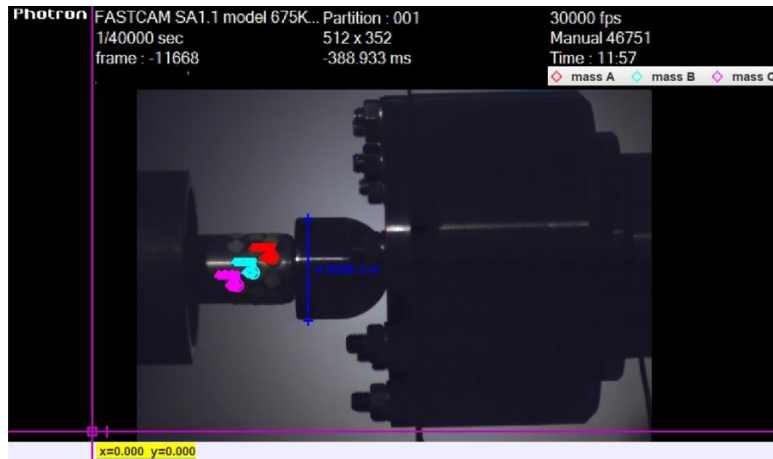


Figure 8. Video image processing

2.2. Numerical study

The numerical study of the experimental tests was performed through LS-DYNA software specialized in modeling the transient nonlinear phenomena [35]. The testing conditions and the geometry allow the use of a simplified model, namely, the problem is formulated 2D axis-symmetric. In Figure 9 the virtual model geometry (2D and 3D) for impactor and plate is illustrated.

The simulation was carried out in six configurations, as follows: impact on an aluminum plate, impact on an aluminum plate with polyurea-polyurethane coating (4 configurations) and impact on two aluminum plates arranged together.

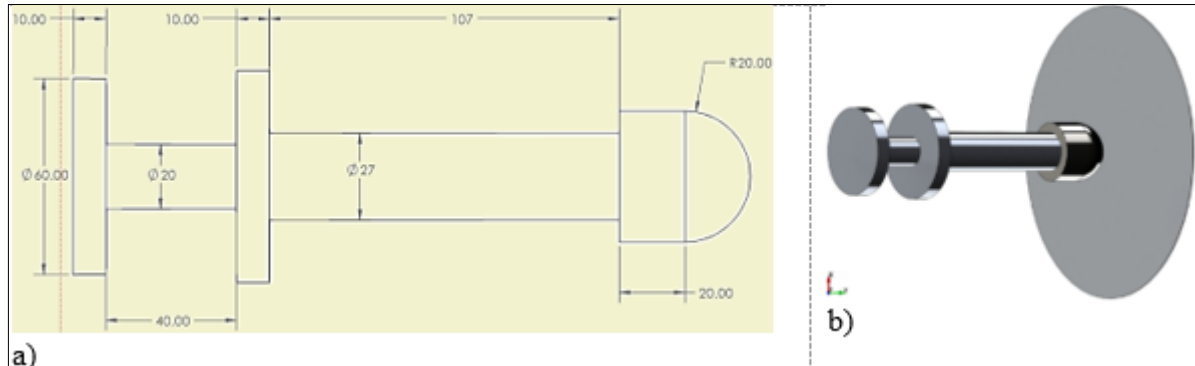


Figure 9. Virtual model geometry: a) specific dimensions, b) 3D model

The geometry of the virtual model is in accordance with the real ones: the impactor has the dimensions presented in Figure 9a and for the aluminum plate a disk with a diameter of 100 mm representing the central circular area of the tested plate was considered.

For the modeled cases, axial symmetric plane elements of SHELL 15 type were used, with weighting of the functions by volume. The discretized domain, with detail in the impact area is illustrated in Figure 10.

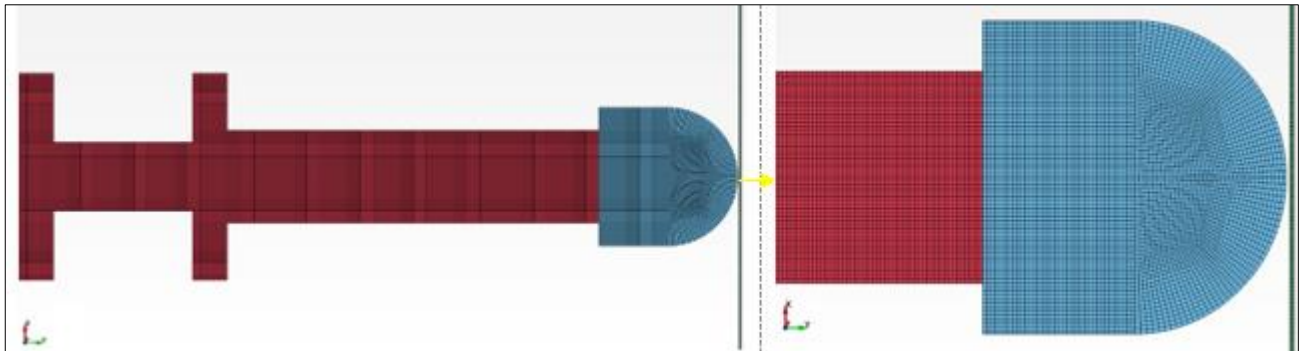


Figure 10. Shape-headed impactor discretization with a detail on the impact area

The mesh is structured with a total number of 12778 elements and 13389 nodes, having a finer discretization in the impact area of the hemispherical shape impactor head.

The impact is simulated by imposing the values of the impact velocities on all the nodes corresponding to the impactor geometry.

The target plates were constrained on the exterior contours in order to replicate the test set-up.

The contact between the component elements of the model was achieved by imposing the "CONTACT_2D_AUTOMATIC_SURFACE_TO_SURFACE" contact condition.

The material models introduced in the program for simulated structures are: for aluminum plate, a material model of type *MAT_PLASTIC_KINEMATIC, and for the polyurea-polyurethane coated on the back of the aluminum plate (for all 4 cases), a material model of type *MAT_OGDEN_RUBBER.

No erosion or failure criteria were used for either material types.

In both cases, were used the material constants presented in [20] and the true stress-true strain curves presented in Figure 3.

3. Results and discussions

All the results obtained from the laboratory test analysis (force sensor, 3D Scan and video processing) are presented in relation with the results from the numerical study.

From the experimental tests, the maximum force is obtained for both approaches, and in terms of deformation, from the 3D Scan processing the residual deformation is obtained and from the video processing the maximum deformation.

Two representative examples of the maximum force evolution obtained by force sensor and by analytically processed data from video processing (velocity time derivation and second principle of mechanics) are presented in Figure 11. It is observed that the curve of force evolution has an ascending trend with oscillations.

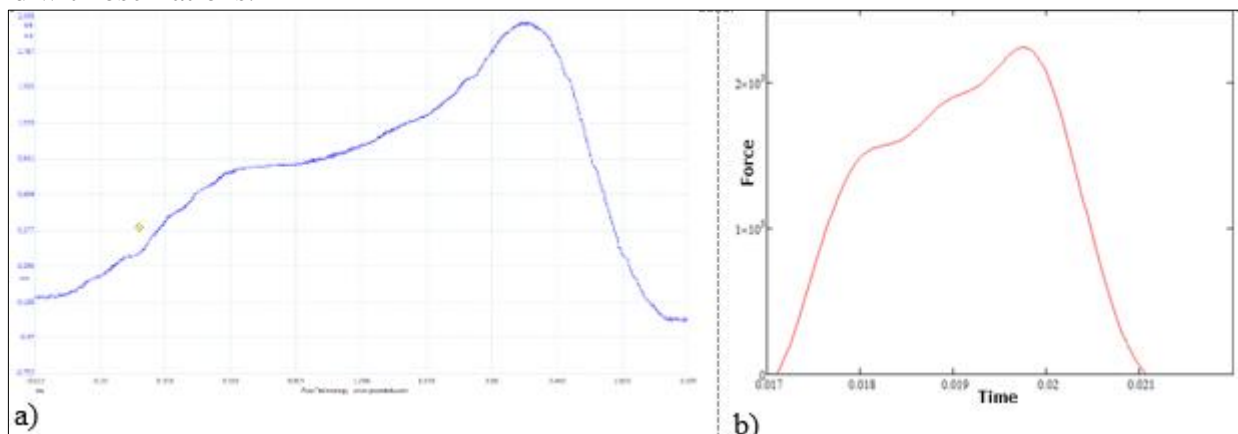


Figure 11. Force evolution (standard plate): a) registered by force sensor, b) processed with the Mathcad software from the video footage

Regarding the tested plates behavior, it is observed that an identical deformation pattern is obtained in the following cases (Table 1):

- 0.2 bar pressure on SA plate – deformation but no fissures;
- 0.4 bar pressure on the multilayer plate, SA+PU – deformation but no fissures;
- 0.6 bar pressure on the multilayer plate, SA+PU-NC3 – deformation but no fissures.

From the images with the deformation patterns, it can be observed that for the multilayer configurations the damage of the aluminum plate is reduced and the polyurea-polyurethane layer absorbs the kinetic energy of the impactor and reduce the degree of plates deformation.

Furthermore, aluminum plates coated with polyurea-polyurethane-MWCNTs nanocomposite configuration allows the metal plate to withstand a load two times higher in terms of kinetic energy.




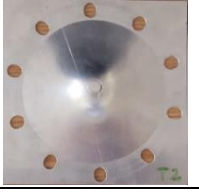




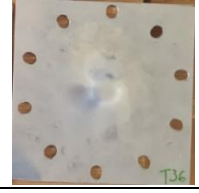


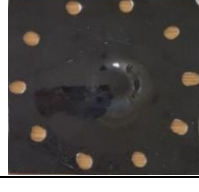

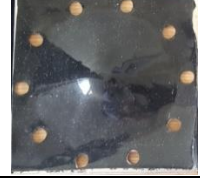







It can be noticed the behavior of multilayer plates when higher deformation and the cracking process and fracture appears. Both aluminum plate coated with polyurea-polyurethane 0.2% carbon nanotubes and double aluminum plate suffered a complete perforation at an approximate velocity value of 14 m/s.

In Table 2 are given the main parameters measured: velocity, deformation and force. The same data are presented in a graphical manner in Figures 12-14. The curves are divided in two groups: SA, SA+PU and DA, and SA + PU, SA + PU-NC2, SA + PU-NC3 and SA + PU-NC4, for each type of measurement and parameter of interest.

It can be seen that the maximum force increases along with the impact velocity until the cracks occur. No significant increase is observed after this threshold, regardless of the type of configuration subjected to the impact.

Moreover, the measured results are in good accordance with data obtained from image processing until the above-mentioned threshold is reached.

Table 1. Deformation patterns after impact loading [5]

Aluminum plate (SA)	Al. plate + PU	Al. plate + PU-NC2	Al. plate + PU-NC3	Al. plate + PU-NC4	Double Al. plate (DA)
0.2 bar					
					
0.3 bar					
					
0.4 bar					
					
0.5 bar					
					

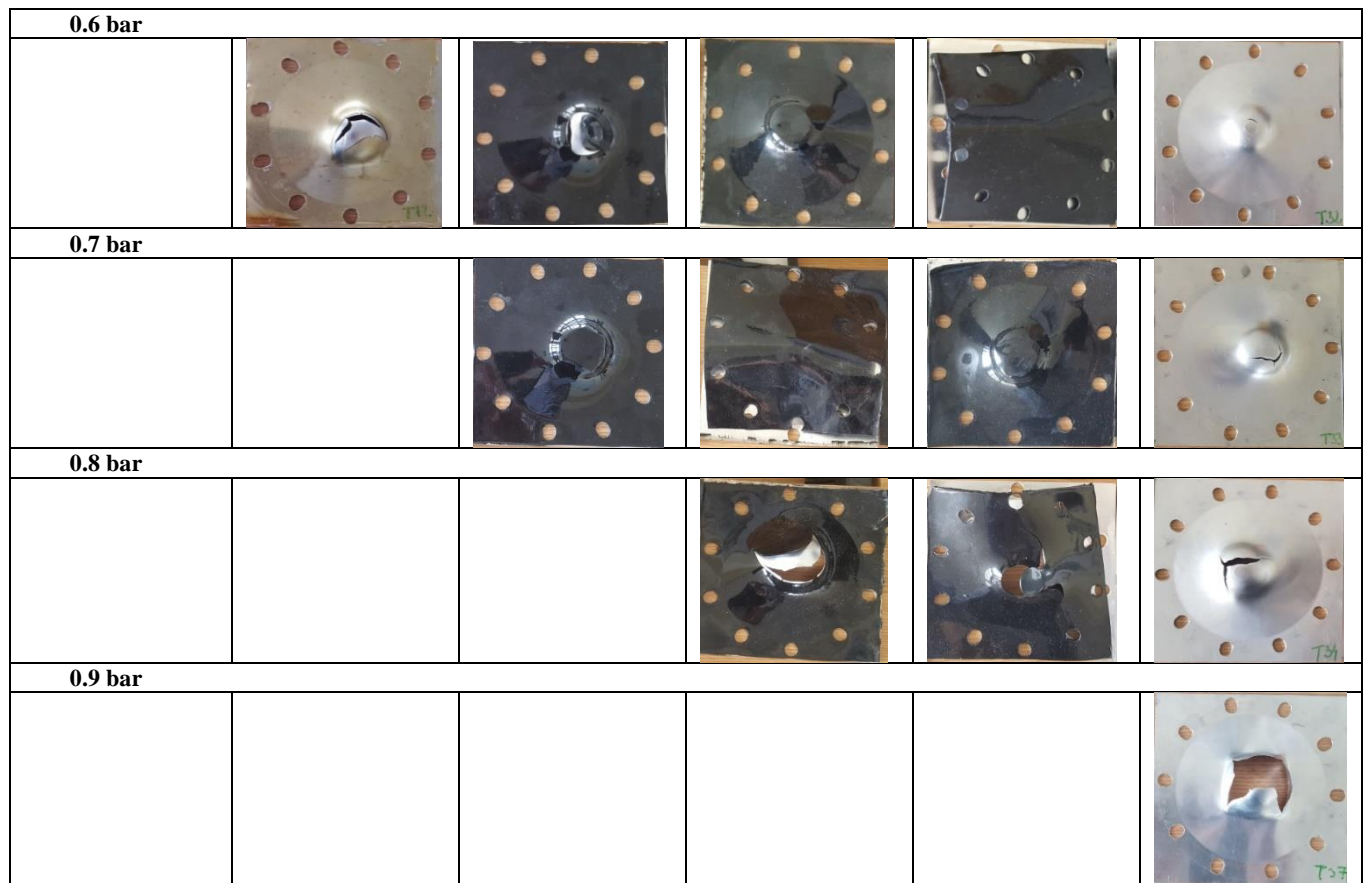


Table 2. Important parameters values at the impact loading from experimental study

Parameters		Aluminum plate (SA)	Al. plate + PU	Al. plate + PU-NC2	Al. plate + PU-NC3	Al. plate + PU-NC4	Double Al. plate (DA)
0.2 bar							
Velocity (m/s)		5.63	5.81	5.62			
Deformation (mm)	3D Scan	9.87	9.64	9.35			
	Video	9.98	9.85	9.69			
Force (KN)	Sensor	2	2	2.1			
	Video	2.38	2.43	2.39			
0.3 bar							
Velocity (m/s)		7.33	7.29	7.1	6.93	7.00	7.39
Deformation (mm)	3D Scan	13.4	12.75	12.25	12.1	12.06	8.75
	Video	13.57	13.09	12.54	12.5	12.62	9.48
Force (KN)	Sensor	2.6	3.0	2.8	2.3	2	3.22
	Video	2.92	3.1	3.02	2.78	3.07	3.7
0.4 bar							
Velocity (m/s)		8.99	9.03	9.2	9.03	8.97	9.02
Deformation (mm)	3D Scan	20.19	15.31	15.43	14.54	14.93	13.04
	Video	20.55	15.92	15.79	16.16	15.97	13.26
Force (KN)	Sensor	2.5	3.6	3.8	3.8	4.0	4.28
	Video	2.61	3.78	3.96	3.88	4.14	4.74
0.5 bar							
Velocity (m/s)		9.23	10.67	10.82	10.73	10.63	10.66
Deformation (mm)	3D Scan	22.38	17.18	17.02	18.06	17.02	13.13
	Video	23	18.24	17.48	18.26	17.31	14.87
Force (KN)	Sensor	1.8	4.1	4.3	5.0	4.4	4.97
	Video	2.7	4.29	4.5	4.64	4.58	5.66



0.6 bar								
Velocity (m/s)				11.93	11.86	10.7	11.68	11.63
Deformation (mm)	3D Scan			21.01	20.4	17.64	19.03	15.03
	Video			21.13	20.8	18.59	19.45	16.22
Force (KN)	Sensor			3.6	3.9	4.1	4.8	5.47
	Video			4.39	4.46	4.43	4.95	6.11
0.7 bar								
Velocity (m/s)					12.98	13.16	12.9	13.12
Deformation (mm)	3D Scan				18.99	20.88	18.19	17.67
	Video				20.66	21.37	19.97	18.57
Force (KN)	Sensor				4.03	4.54	4.0	6.45
	Video				4.75	5.16	4.9	6.35
0.8 bar								
Velocity (m/s)						14.23	13.98	14.1
Deformation (mm)	3D Scan					22.81	P	20.95
	Video					23.97	P	21.77
Force (KN)	Sensor					4.4	4.1	6.19
	Video					4.9	4.66	5.88
0.9 bar								
Velocity (m/s)								14.41
Deformation (mm)	3D Scan							P
	Video							P
Force (KN)	Sensor							6.32
	Video							5.97

P – Complete perforation.

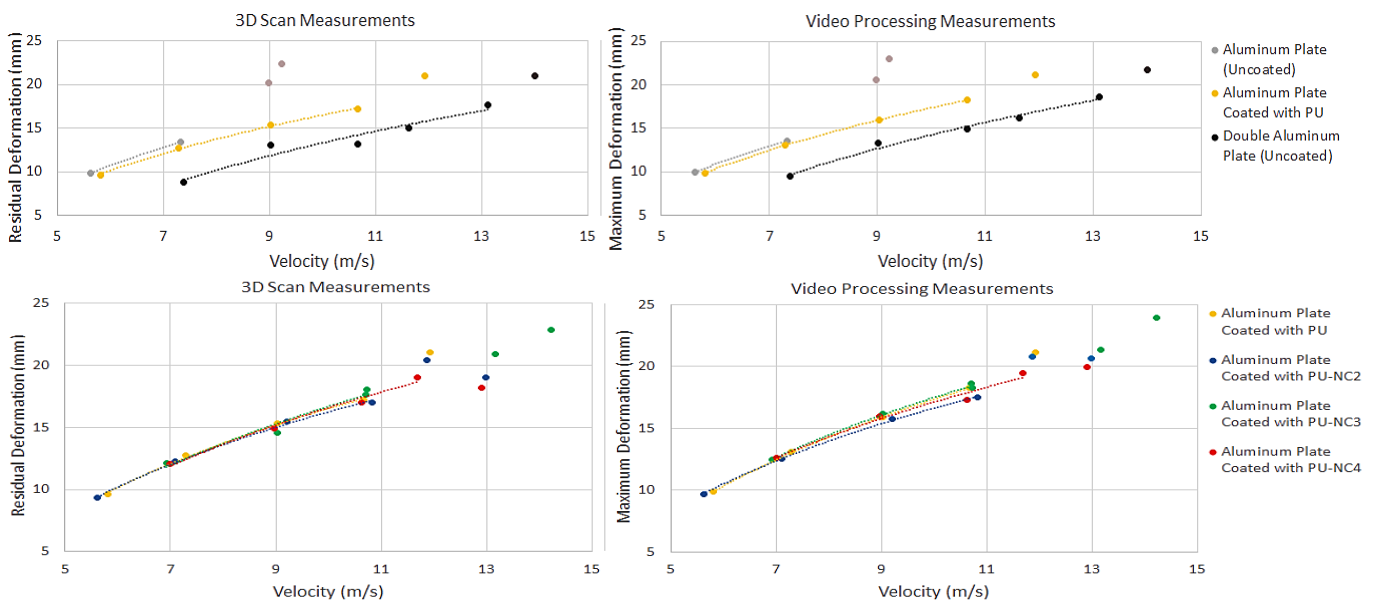
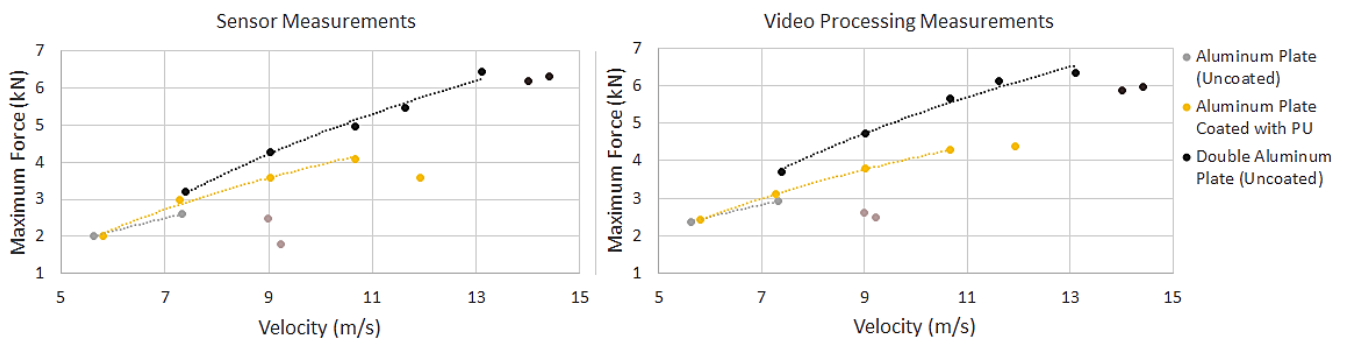


Figure 12. Comparative evolution of deformation – velocity curve



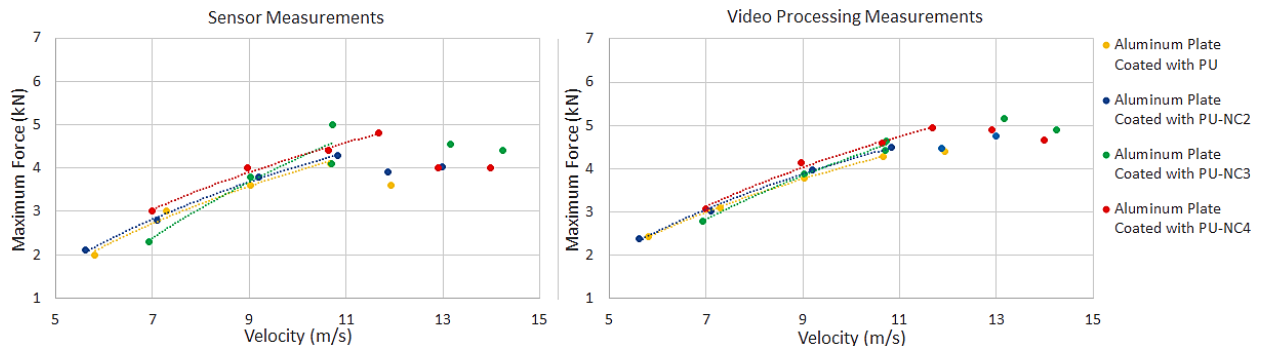


Figure 13. Comparative evolution of maximum force – velocity curve

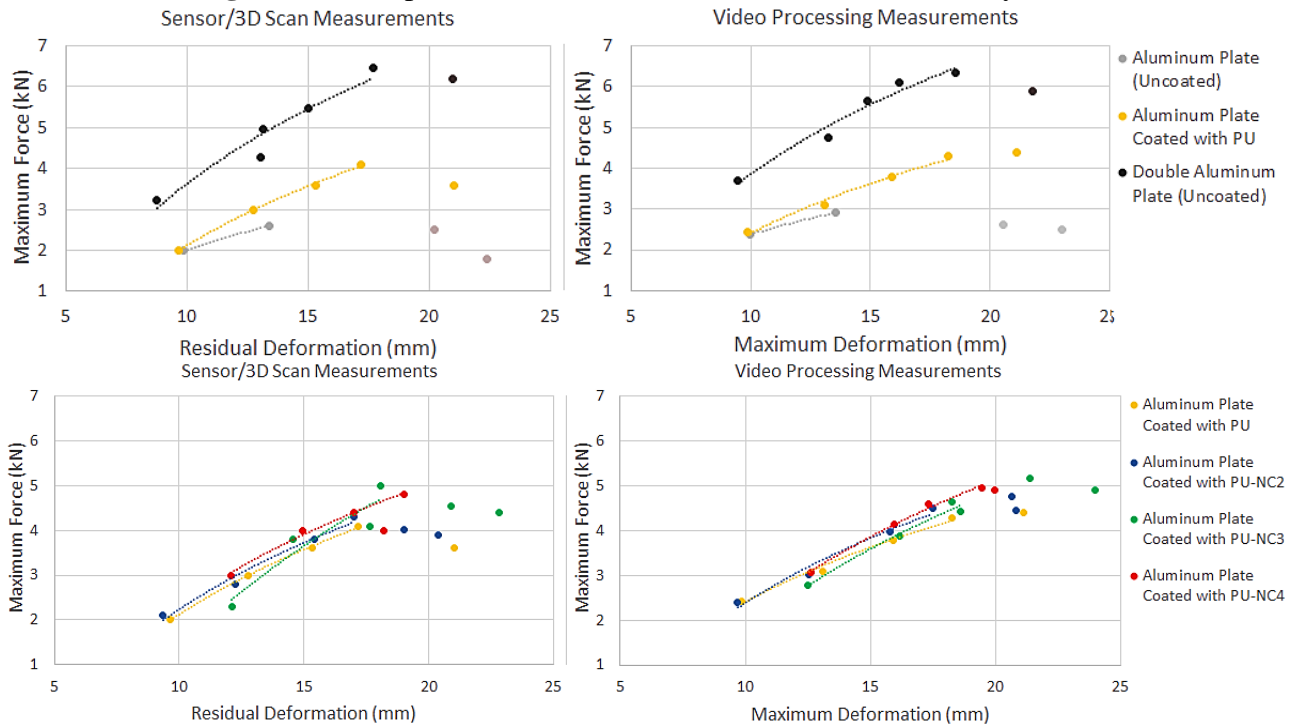


Figure 14. Comparative evolution of maximum force – deformation curve

Regarding the numerical simulation, the constraints and contact chosen allow to observed both loading and unloading phases. In Figure 15 is presented the Al. plate + PU-NC3 model for the maximum plate deformation and a subsequent moment when the impactor is no longer in contact with the plate.

Based on the simulation results, the time-dependent variations of the velocity and acceleration of the impactor were recorded, as well as the displacement of a node from the tested configuration for all simulated scenarios. Typical curves evolutions are given in Figures 16-18. From these curves were extracted the same parameters as those measured in the experimental study (Table 3).

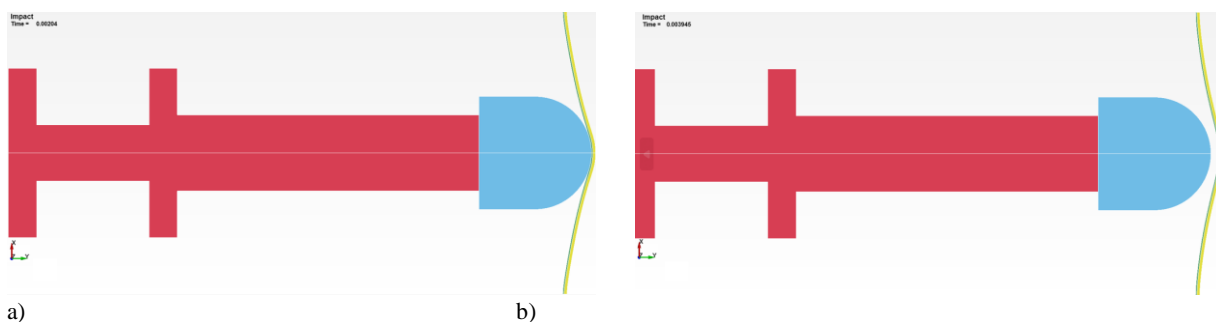


Figure 15. Sequences for impact at 7 m/s velocity for Al. plate + PU-NC3:
 a) maximum plate deformation, b) backward impactor movement

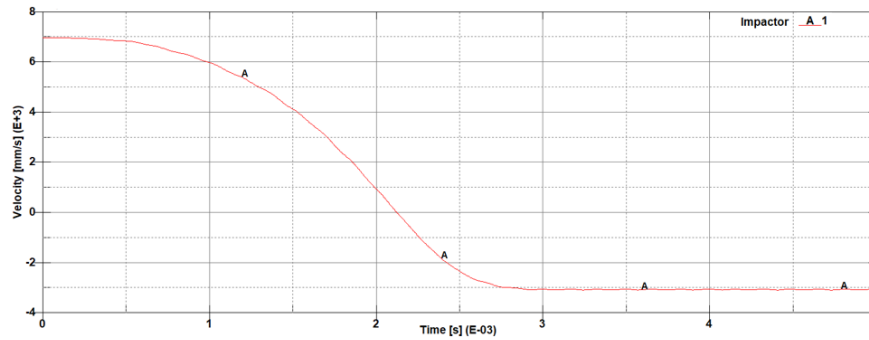


Figure 16. Impactor velocity curve (Al. plate + PU-NC3 – 7 m/s)

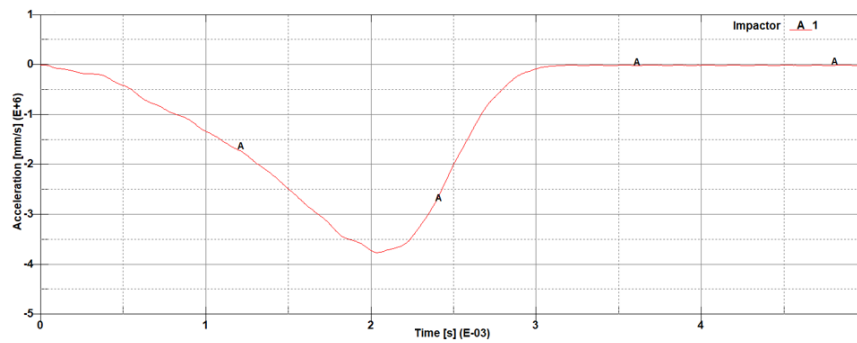


Figure 17. Impactor acceleration curve (Al. plate + PU-NC3 – 7 m/s)

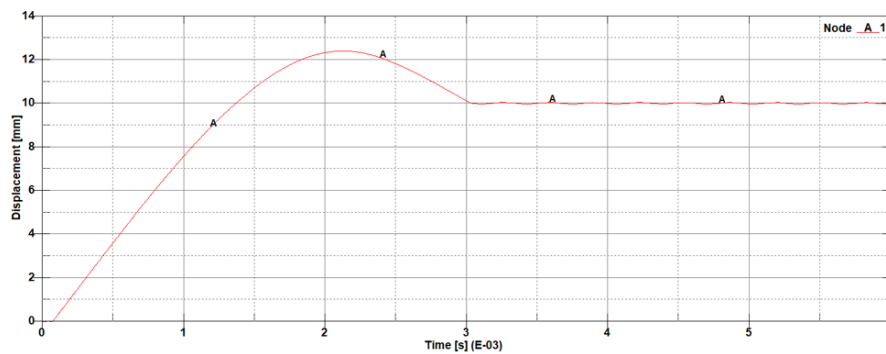


Figure 18. Deformation of plate central point (Al. plate + PU-NC3 – 7 m/s)

Table 3. Important parameters values at the impact from numerical study

Parameters	Aluminum plate	Al. plate + PU	Al. plate + PU-NC2	Al. plate + PU-NC3	Al. plate + PU-NC4	Double Al. plate
Velocity (m/s)	5.6	6	5.6			
Residual Deform. (mm)	11.5	9.85	9.78			
Maximum Deform. (mm)	12	10.2	10.1			
Maximum Force (kN)	2.6	2.82	2.7			
Velocity (m/s)	7.3	7.29	7.1	7	7.0	7.0
Residual Deform. (mm)	14.2	13.1	12.95	10	12.5	10.1
Maximum Deform. (mm)	14.7	13.5	13.2	12.3	12.85	10.6
Maximum Force (kN)	3.6	3.9	3.4	3.0	2.88	4.2
Velocity (m/s)		9.0	9.2	9.0	9.0	9
Residual Deform. (mm)		15.86	15.43	15.06	14.93	13.53
Maximum Deform. (mm)		16.21	15.79	16.8	15.97	13.81
Maximum Force (kN)		4.05	3.8	4.2	4.0	5.3



Velocity (m/s)		10.5	11.0	11.0	10.66	10.66
Residual Deform. (mm)		17.89	17.54	18.96	17.72	14.5
Maximum Deform. (mm)		19.10	18.38	19.66	18.27	15.1
Maximum Force (kN)		4.1	4.3	5.3	4.8	6.8
Velocity (m/s)				10.7	11.7	11.63
Residual Deform. (mm)				18.37	19.64	16.4
Maximum Deform. (mm)				18.94	20.02	17.0
Maximum Force (kN)				4.75	5.03	7.2
Velocity (m/s)						13.12
Residual Deform. (mm)						17.6
Maximum Deform. (mm)						18.3
Maximum Force (kN)						7.8

*For the cases where the total perforation occurs, the numerical simulation was not performed.

First of all, the simulation results in terms of plates deformations are in good agreement with the experimental ones. Nevertheless, the differences between the maximum forces recorded and those calculated are more significant, for example for a single aluminum plate impacted at 7 m/s, the experimental result is value 2.6/2.9 kN and from numerical simulation is 3.6 kN.

These differences may be explained by a possible misalignment between the moving part and the target support where the sensor was mounted. This assumption is sustained also by the differences between the recorded force profiles in time and calculated ones. As it can be seen in Figure 17, no oscillations occur during the loading phase, as long as the simulations deals with an ideal axial configuration.

4. Conclusions

Laboratory impact tests at low velocity in a dynamic regime were performed on aluminum plates coated with Hybrid Polyurea-Polyurethane-MWCNTs Nanocomposites.

These samples have as the main layer an aluminum plate on which a layer of polyurea-polyurethane with different compositions was deposited: simple polyurea-polyurethane and polyurea-polyurethane containing carbon nanotubes in different concentrations.

The experimental study investigation was based on the force sensor recordings, high-speed camera images and 3D scans. While 3D Scans processing highlights the residual deformation, the video images processing allows us to estimate the maximum deformation, a process parameter that cannot be measured with post-test tools.

The maximum force obtained by image processing is in good accordance with the values measured by force sensor as long as no fracture occur in aluminum plates.

The addition of hyperelastic coatings ensures a better resistance of the aluminum plates, the impact velocity at which cracks appear increases, the best results being obtained for the composition with 0,2% carbon nanotubes. The same trend is also observed in the case of the maximum forces recorded during the tests. However, the presence of the hyperelastic layer does not significantly change the maximum deformation supported by the aluminum plates before the appearance of cracks. Nevertheless, an important change is observed regarding the position of the point where the fractures initiate. When hyperelastic coatings are present, the fracture initiation point moves away from the central point with the maximum deformation. The fracture propagation mode also changes. If in the case of a simple plate the initial fracture tends to bifurcate quickly and lead to the formation of petals, when there are hyperelastic coatings the crack propagates in a circular pattern that leads to the formation of a pseudo-plug attached to the plate. These differences can be explained by the influence of the hyperelastic layer on the necking phenomena occurrence and stress triaxiality.

An LS-DYNA numerical study was performed for further investigations. The used material models are proven to be accurate enough to obtain results similar to the experimental ones, in terms of plates deformations. However, in term of maximum force, the results are no longer similar, a mismatch that may be attributed to the lack of collinearity between the impactor and the target's support.

The negative residual velocity, observed both in the experimental and numerical studies, is caused by the elastic component of the plate deformation that disappears during the unloading phase.

The concordance between the results obtained based on image processing and the results obtained through classical methods of measurement and study (sensors, 3D scanning and numerical simulation) shows that the approach proposed in the present work is a viable one.

Acknowledgments: This work is supported by the National Authority for Scientific Research from the Ministry of Education, Research and Youth of Romania through the National Project contract number 278/2014.

References

1. SAI S. SARVA, DESCHANEL, S., BOYCE, M.C., CHEN, W., Stress-strain behavior of a polyurea and a polyurethane from low to high strain rates, *Polymer*, **48**(8), 2007, 2208-2213.
2. RAMAN, S.N., NGO, T., LU, J., MENDIS, P., Experimental investigation on the tensile behavior of polyurea at high strain rates. *Mater. Des.*, **50**, 2013, 124-129.
3. AMINI, M.R., ISAACS, J., NEMAT-NASSER, S., Investigation of effect of polyurea on response of steel plates to impulsive loads in direct pressure-pulse experiments. *Mech. Mater.*, **42**, 2010, 628-639.
4. TOADER, G., DIACON, A., AXINTE, S.M., MOCANU, A., RUSEN, E., State-of-the-Art Polyurea Coatings: Synthesis Aspects, Structure-Properties Relationship, and Nanocomposites for Ballistic Protection Applications. *Polymers*, **16**, 2014, 454.
5. ***Raport stiintific și tehnic, Contract nr. 278/2014, Sistem de Protectie Antiexplozie pentru Echiparea Vehiculelor, Etapa de executie 2017.
6. ROLAND, C.M., FRAGIADAKIS, D., GAMACHE, R.M., Elastomer-steel laminate armor, *Composite Structures*, **92**(5), 2010, 1059-1064.
7. FINDIK, F., TARIM, N., Ballistic impact efficiency of polymer composites. *Compos. Struct.*, **61**, 2003, 187-192.
8. ÁVILA, A.F., NETO, A.S., NASCIMENTO, H., JR., Hybrid nanocomposites for mid-range ballistic protection. *Int. J. Impact Eng.*, **38**, 2011, 669-676.
9. IFTIMIE, B., LUPOAE, M., ORBAN, O., Experimental Investigations Regarding the Behavior of Composite Panels Based on Polyurea and Kevlar or Dyneema Layers Under Blast and Fragments, *Mater. Plast.*, **56**(3), 2019, 538-542.
10. ROTARIU, A., BUCUR F., TOADER, G., LUPOAE M., SAVA, A., ȘOMOIAG, P., CIRMĂCI-MATEI, M.V., Experimental Study on Polyurea Coating Effects on Deformation of Metallic Plates Subjected to Air Blast Loads, *Mater. Plast.*, **53**(4), 2016, 670-674.
11. BUCUR, F., TRANĂ, E., ROTARIU, A., Numerical and experimental study on the locally blast loaded polyurea coated steel plates, *Mater. Plast.*, **56**(3), 2019, 492-499.
12. S. N. RAMAN, T. NGO, P. MENDIS, T. PHAM, Elastomeric Polymers for Retrofitting of Reinforced Concrete Structures against the Explosive Effects of Blast, *Adv. in Mater. Science and Eng.*, **2012**, 754142, 2012.
13. HE, C., LIU, Y., YAO, Y., CHEN, Q., Experimental and Numerical Investigation of Ballistic Resistance of Polyurea-Coated Aluminum Plates under Projectile Impacts, *Crystals*, **13**, 2023, 1039.
14. HUANG, X.L., ZHANG, W., DENG, Y.F., JIANG, X.W., Experimental investigation on the ballistic resistance of polymer-aluminum laminated plates, *Int. J. Impact Eng.* 2018.
15. MOHOTI, D., NGO, T., RAMAN, S.N., ALI, M., MENDIS, P., Plastic deformation of polyurea coated composite aluminium plates subjected to low velocity impact. *Mater. Des.* 2014, **56**, 696-713.
16. MOHOTI, D., NGO, T., MENDIS, P., RAMAN, S.N., Polyurea coated composite aluminium plates subjected to high velocity projectile impact. *Int. J. Mater. Des.*, **52**, 2013, 1-16.
17. MOHOTI, D., NGO, T., RAMAN, S.N., MENDIS, P., Analytical and numerical investigation of polyurea layered aluminium plates subjected to high velocity projectile impact, *Mater. Design.*, **82**, 2015, 1-17.



18. WANG, Y., DING, L., LIN, J., QIU, X., WU, C., LIU, C., TIAN, Y., ZHANG, R., HUANG, W., MA, M., Recent Developments in Polyurea Research for Enhanced Impact Penetration Resistance and Blast Mitigation, *Polymers*, **16**, 2024, 440.
19. TOADER, G., MOLDOVAN, A.E., DIACON, A., F.M. DIRLOMAN, E. RUSEN, A. PODARU, T. ROTARIU, GINGHINA, R.E., HOZA, O.E., Effect of Aromatic Chain Extenders on Polyurea and Polyurethane Coatings Designed for Defense Applications, *Polymers*, **15**(3), 2023, 756.
20. TOADER, G., DIACON, A., RUSEN, E., RIZEA, F., TEODORESCU, M., STĂNESCU, P.O., DAMIAN, C., ROTARIU, A., TRANĂ, E., BUCUR, F., A Facile Synthesis Route of Hybrid Polyurea-Polyurethane-MWCNTs Nanocomposite Coatings for Ballistic Protection and Experimental Testing in Dynamic Regime, *Polymers*, **13**, 2021, 1618.
21. NANTASETPHONG, W., AMIRKHIZI, A.V., JIA, Z., NEMAT-NASSER, S., Polyurea-Based Composites: Ultrasonic Testing and Dynamic Mechanical Properties Modeling, *Conference Proceedings of the Society for Experimental Mechanics Series*. Springer, 2013.
22. BUCUR, F., TRANĂ, E., ROTARIU, A., GAVRUS A., BARBU, C., GUINES, D., Experimental and numerical analysis concerning the behaviour of OL50 steel grade specimens coated with polyurea layer under dynamics loadings, *EPJ Web of Conferences*, **94**, 2015, 04044.
23. ROTARIU, A., TRANĂ, E., MATAACHE, L., CIRMACI-MATEI, M., SANDU, S., MOLDOVEANU, C., BUCUR, F., Experimental Study on the Dynamic Response of Polyurethane/fly Ash Ceramic Foam, *Mater. Plast.*, **58**(1), 2021, 106-112.
24. BACIU, C., LUPOAE, M., CONSTANTIN, D., Experimental analysis on reduced-scale protective doors, *WIT Transactions on the Built Environment*, **180**, 2018, 101-111.
25. BUCUR, F., ROTARIU, A., MATAACHE, L., BACIU, F., JIGA, G., TRANĂ, E. Experimental and numerical study on the behavior of Dyneema® HB26 composite in compression, *Materiale Plastice*, **57**(2), 2020, 113-122.
26. CERBU, C., URSACHE, ȘT., BOTIȘ, M. F., HADĂR, A., Simulation of the Hybrid Carbon-Aramid Composite Materials Based on Mechanical Characterization by Digital Image Correlation Method, *Polymers*, **13**(23), 2021, 4184.
27. TUDOR, D.I., PETRESCU, H.-A., HADĂR, A., ROȘU, D., Computer Tomography Investigation of Defects in Plastic Material Plates, *Mater. Plast.*, **49**(2), 2012, 123-128.
28. MOHAGHEGHIAN, I., MCSHANE, G.J., STRONGE, W.J., Quasi-static and impact perforation of polymer-metal bi-layer plates by a blunt indenter. *Thin Walled Struct.*, **117**, 2017, 35–48.
29. SHIM, J., MOHR, D., Punch indentation of polyurea at different loading velocities: Experiments and numerical simulations, *Mechanics of Materials*, **43**(7), 2011, 349-360.
30. LIU, Q, WANG, S.P., LIN, X., CUI, P., ZHANG, S., Numerical simulation on the anti-penetration performance of polyurea-core Weldox 460 E steel sandwich plates. *Compos. Struct.* **236**, 2020, 111852.
31. MOHOTTI, D.; FERNANDO, P.L.N.; WEERASINGHE, D.; REMENNIKOV, A. Evaluation of effectiveness of polymer coatings in reducing blast-induced deformation of steel plates. *Def. Technol.*, **17**, 2021, 1895–1904.
32. ILIESCU, N., ATANASIU, C., HADĂR, A., The simulation of the mechanical behaviour of engineering structures on models made of plastic materials with special properties, *Mater. Plast.*, **42**(1), 2005, 72-76.
- 33.***<https://www.creaform3d.com/en/news/creaform-adds-academia-20-3d-scanner-its-educational-solution-suite>
34. ***<https://proto3000.com/product/goscan-3d/>
- 35.***LS-Dyna Keyword users's manual 971

Manuscript received: 05.03.2024